Cholesterol loading in macrophages stimulates formation of ER-derived vesicles with elevated ACAT1 activity

Naomi Sakashita,[1,*,†] Catherine C. Y. Chang,[†] Xiaofeng Lei,[*] Yukio Fujiwara,[*] Motohiro Takeya,[*] and Ta-Yuan Chang[1,†]

Department of Cell Pathology,* Graduate School of Medical Sciences, Kumamoto University, Kumamoto 861-8556, Japan; and Department of Biochemistry,† Dartmouth Medical School, Hanover, NH 03755

Abstract **ACAT1 is normally a resident enzyme in the endoplasmic reticulum (ER). We previously showed that treating macrophages with denatured LDL causes a large increase in ER-derived, ACAT1-positive vesicles. Here, we isolated ER membranes and ER-derived vesicles to examine their ACAT enzyme activity in vitro. The results showed that when macrophages are grown under normal conditions, ACAT1 is located in high density ER membrane; its enzymatic activity is relatively low. Loading macrophages with cholesterol did not increase the total cellular ACAT1 protein content significantly but caused more ACAT1 to appear in ER-derived vesicles. These vesicles exhibit lower density and are associated with markers of both ER and the trans-Golgi network. When normalized with equal ACAT1 protein mass, the enzymatic activities of ACAT1 in ER-derived vesicles were 3-fold higher than those present in ER membrane. Results using reconstituted ACAT enzyme assay showed that the increase in enzyme activity in ER-derived vesicles is not due to an increase in the cholesterol content associated with these vesicles. Overall, our results show that macrophages cope with cholesterol loading by using a novel mechanism: they produce more ER-derived vesicles with elevated ACAT1 enzyme activity without having to produce more ACAT1 protein.**—Sakashita, N., C. C. Y. Chang, X. Lei, Y. Fujiwara, M. Takeya, and T-Y. Chang. **Cholesterol loading in macrophages stimulates formation of ER-derived vesicles with elevated ACAT1 activity.** ***J. Lipid Res.*** **2010.** 51: **1263–1272.**

Supplementary key words foam cells • atherosclerosis • low-density lipoprotein

In mammalian cells, the cholesterol content in various membranes varies from the highest in the plasma membrane to the lowest in the endoplasmic reticulum (ER) membrane. Excess cellular cholesterol is converted to cholesteryl esters or is removed from cells by cellular cholesterol efflux (1, 2). The conversion of free cholesterol to cholesteryl ester is catalyzed by the enzyme ACAT. Two ACAT isoforms exist in mammals: ACAT1 and ACAT2 (3–5). ACAT1 is ubiquitously expressed in various tissues, while ACAT2 is mainly expressed in intestinal enterocytes and in hepatocytes (5–7). Macrophages play key roles in atherosclerosis. Under hyperlipidemic conditions, macrophages continuously internalize denatured/modified LDL. Cholesterol derived from internalized lipoproteins is converted to cholesteryl esters by ACAT1, the major ACAT isozyme in macrophages (8). Chronic exposure to denatured/modified LDL causes macrophages to become foamy in appearance; foamy macrophages are hallmarks of early atherosclerotic lesions. In advanced lesions, in addition to cholesteryl esters, free (unesterified) cholesterol also accumulates in macrophages. The excessive buildup of free cholesterol in membranes can cause cellular toxicity, especially in macrophages (9, 10). In various cell types examined, ACAT1 is mainly located in the tubular ER (11); in mouse macrophages and other cell types examined, 5–15% of the total immunoreactive ACAT1 signal is also present in ER-derived, perinuclear structure(s) near the *trans*-Golgi network (TGN) and the endocytic recycling compartment (12). In human macrophages, when maintained in normal medium, the ACAT1 signal is mainly with the tubular ER; however, adding modified LDL to the growth medium of these cells caused up to 30–40% of the total ACAT1 immunoreactive signals to become associated with small, ER-derived vesicles 80–100 nm in diameter (13). These studies suggest that in macrophages, ACAT1 can be associated with ER-derived vesicles, especially when cells are grown in cholesterol-rich conditions. These ACAT1-positive, ER-derived structures had not previously been isolated in vitro. In the current work, we used OptiPrep gradient ultracentrifugation to isolate various ACAT1-

This work was supported by the National Institutes of Health Grants HL-60306 and HL-36709 (to T-Y.C.) and by Grant-in-Aid for Scientific Research B-17390115 (to N.S.) and B-16390108 (to M.T.) from the Japan Society for Promotion of Science. Its contents are solely the responsibility of the authors and do not necessarily represent the official views of the National Institutes of Health or other granting agencies.

Manuscript received 9 June 2009 and in revised form 1 July 2009.

Published, JLR Papers in Press, July 1, 2009
DOI 10.1194/jlr.M900288-JLR200

Abbreviations: ER, endoplasmic reticulum; TGN, trans-Golgi network; mβCD, 2-methyl-β-cyclodextrin.

[1]To whom correspondence should be addressed.
e-mail: Ta.Yuan.Chang@Dartmouth.EDU (T-Y.C.);
nanaomi@gpo.kumamoto-u.ac.jp (N.S.)

positive membrane fractions and evaluated the ACAT enzyme activities in these fractions.

MATERIALS AND METHODS

Materials

FBS, RPMI1640 medium, protease inhibitor cocktail, SDS, 2-methyl-β-cyclodextrin (mβCD), paraformaldehyde, BSA, saponin, primulin, and PMA were from Sigma. Penicillin-streptomycin solution was from Invitrogen. DTT and SuperSignal Chemiluminescent substrate were from Pierce. ProLong Antifade kit, anti-rabbit IgG Alexa Fluor 488, and anti-mouse IgG Alexa Fluor 568 were from Molecular Probes. The rabbit anti-human ACAT1 antibodies (DM10 and DM102) and the mouse anti-human ACAT1 monoclonal antibody were as previously described (14, 15). Monoclonal antibodies against syntaxin 6, calnexin, BiP, and GM130 were from BD Biosciences. Monoclonal antibody against sodium/potassium ATPase (Na/K ATPase) was from Upstate USA Inc. Iodixanol solution (OptiPrep) used to prepare density gradient was from Axis-Shield. Pansorbin beads for the immunoadsorption experiment were from Calbiochem. [^{3}H]oleyl-CoA was prepared as described previously (15). The ACAT1 specific ACAT inhibitor K-604 was a generous gift from Kowa Co. Ltd. (Tokyo, Japan) (16). LDL (density of 1.019–1.063 g/ml) and acetylated LDL were prepared from fresh human plasma as previously described (8). Aggregated LDL was prepared by vortex mixing LDL at maximal speed for 2 min as described previously (17).

Cell line and cell culture. Human monocytic cell line THP-1 was from ATCC. THP-1 cells were maintained in 150 mm dishes in medium A (RPMI1640 medium plus 10% FBS, 100 units/ml penicillin G, and 0.1 mg/ml streptomycin sulfate). THP-1 cells treated with 100 nM PMA in medium A for 7 days were used for experiments described here. Human monocytes were isolated from blood of healthy volunteers. Informed written consent was obtained from all volunteers in accordance with protocols approved by the Kumamoto University Hospital Review Board. Monocyte-derived macrophages, grown in medium A in 150 mm dishes for 9 days, were used. Cholesterol-rich macrophages were prepared by incubating macrophages with medium A containing 100 μg/ml of aggregated LDL, 100 μg/ml of acetylated LDL, or 250 μM of mβCD containing 16 μM cholesterol (mβCD/cholesterol complex) for 48 h.

Methods

Immunoblot analysis. SDS (at 10% final) and DTT (at 0.1 M final) were added to OptiPrep fractions, immunoadsorbed samples, or whole cell lysates. After incubation at 37°C for 30 min, the solubilized proteins were analyzed by10% SDS-PAGE and subjected to immunoblotting as described previously (14).

Cellular cholesterol and cholesteryl ester contents. THP-1 and human macrophages grown in 6-well tissue culture plate with medium A with or without various additional cholesterol sources for 48 h were rinsed with PBS three times and dried at room temperature, then treated with 2 ml/well of hexane:2-propanol (3:2). The total cholesterol and free cholesterol contents present in the lipid extracts were determined by using the cholesterol determination kit following the manufacturer's instruction (Wako Chemical, Tokyo, Japan). The cholesteryl ester values were calculated by subtracting the free cholesterol values from the total cholesterol values. Cellular protein dissolved in 0.1 N sodium hydroxide was determined by using a BCA Protein Assay kit (Pierce) with BSA as a standard.

Immunoisolation of ACAT1-containing membranes. Immunoadsorption was employed to isolate ACAT1-positive membranes using the procedure briefly described below: 30 μL of precleaned pansorbin beads were incubated with 6 μg of rabbit polyclonal ACAT1 antibodies DM102 or nonimmunized rabbit IgG in buffer for 2 h at 4°C. After washing, the beads were incubated with ACAT1-rich OptiPrep fraction in buffer containing 100 mM sodium chloride for 15 h at 4°C. After brief centrifugation in a microfuge, the pellet was isolated and washed thoroughly.

Immunostaining and confocal microscopy. Cells cultured in a 6-well tissue culture plate with sterile coverslips were washed with Buffer A [PBS (pH 7.2) containing 0.5% BSA and 0.01% saponins] and were fixed with 4% paraformaldehyde in 0.1 M phosphate buffer (pH 7.4) on ice for 30 min. After washing, the samples were pretreated with 5% goat serum and incubated with primary antibodies for 60 min, then incubated with anti-rabbit Alexa Fluor 488 and anti-mouse Alexa Fluor 568 for 60 min and scanned and recorded as digital images using Carl Zeiss LSM510 Meta or Olympus FV300 at a resolution of 1,024 × 1,024 pixels/frame using an objective lens with numerical aperture 1.40 and estimated optical thickness < 500 nm. For quantitative analysis of confocal images, at least 30 images were scanned at random; the colocalization coefficient between ACAT1 signal and various organelle markers as indicated were calculated by using the WinROOF image analysis software, version 5.7. Statistical analysis was carried out by performing Mann-Whitney U-test; P-values < 0.05 were considered statistically significant.

Subcellular fractionation. Experiments were performed at 4°C. Cells grown in a 150 mm plate were scraped off into 1 ml homogenization buffer containing 0.25 M sucrose, 20 mM Tris buffer (pH 7.8), and protease inhibitor cocktail and were homogenized using a stainless steel tissue grinder (Dura-Grind, Wheaton). The postnuclear supernatant was loaded onto the top of a 9 ml, continuous 7.5–19.5% OptiPrep gradient in homogenization buffer and was fractionated by sedimentation velocity ultracentrifugation in a SW41 rotor at 200,000 *g* for 2 h; 19 equal fractions were collected from top to bottom. To perform the two-step sequential fractionation method, after the first step centrifugation, OptiPrep was added to the low-density, ACAT1-rich fraction (fraction 4) to reach 20% final concentration in 1 ml. The sample was placed at the bottom of a continuous 7.5–19.5% OptiPrep gradient and centrifuged at 200,000 *g* for 2 h. Afterwards, 19 equal fractions were collected from top to bottom.

ACAT enzyme assays. Each OptiPrep membrane fraction was used directly for ACAT enzyme activity determination using the nonreconstituted assay; in this assay, the cellular cholesterol associated with the membrane served as the enzyme substrate (15, 18). In addition, in Fig. 2E, each membrane fraction was subjected to ACAT activity determination using both the nonreconstituted assay and the reconstituted vesicle assay. In the latter assay, the cholesterol present in the reconstituted vesicles serves as the enzyme substrate (15, 18). To briefly describe the latter assay, each membrane fraction was first treated with the detergent 2% CHAPS and 1 M potassium chloride; ACAT solubilized in detergent was reconstituted into vesicles by diluting the detergent treated extract into a large excess of preformed phospholipid vesicles with defined cholesterol/phosphatidylcholine molar ratio (at 0.2). For each assay employed, the assay was initiated by adding 20 μL of solution containing 10 nmol of [^{3}H]oleoyl-CoA and 10 nmol of fatty acid-free BSA, and the reaction mixture was incubated at 37°C for up to 30 min. The enzyme activity was linear with time within 30 min. The ACAT1-specific ACAT inhibitor K-604 was employed at final concentration of 1 μM (16).

RESULTS

The cholesterol/cholesteryl ester content and the ACAT1 protein content of THP-1 macrophages and human primary macrophages

We treated macrophages with aggregated LDL or with other cholesterol donors to promote foam cell formation in vitro. When PMA-activated THP-1 cells were treated with various cholesterol donors for 48 h, cellular free cholesterol content increased from 10.3 to 23.0 (acetylated LDL), 23.4 (aggregated LDL), or 19.9 (mβCD/cholesterol complex) μg/mg cellular protein; cellular cholesteryl ester content increased from 8.0 to 79.6 (acetylated LDL), or 120 (aggregated LDL), or 121 (mβCD/cholesterol complex) μg/mg protein (**Fig. 1A**, left panels). Likewise, when primary human macrophages grown in medium A were treated with aggregated LDL, cellular cholesterol content increased from 10.4 to 34.1 μg/mg protein; cholesteryl ester content increased from 5.1 to 148 μg/mg protein (Fig. 1A, right panels). After 48 h of aggregated LDL treatment, the protein content of ACAT1 was modestly increased in the THP-1 macrophages but not in the primary human macrophages (Fig. 1B).

The density and enzyme activity of the ACAT1-positive membranes in THP-1 macrophages

We next employed subcellular fractionation to isolate the ACAT1-containing membranes in THP-1 macrophages. The results showed that in basal "medium A" conditions, most of the ACAT1 signal appeared in the medium-density fractions (fractions 8–11) where the ER marker protein calnexin and the TGN marker protein syntaxin 6 were found (**Fig. 2A**). In contrast, after incubating cells with aggregated LDL, most of the ACAT1 signal and the calnexin signal shifted to lower-density fractions (fractions 4–7); interestingly, a significant portion of the syntaxin 6 signal

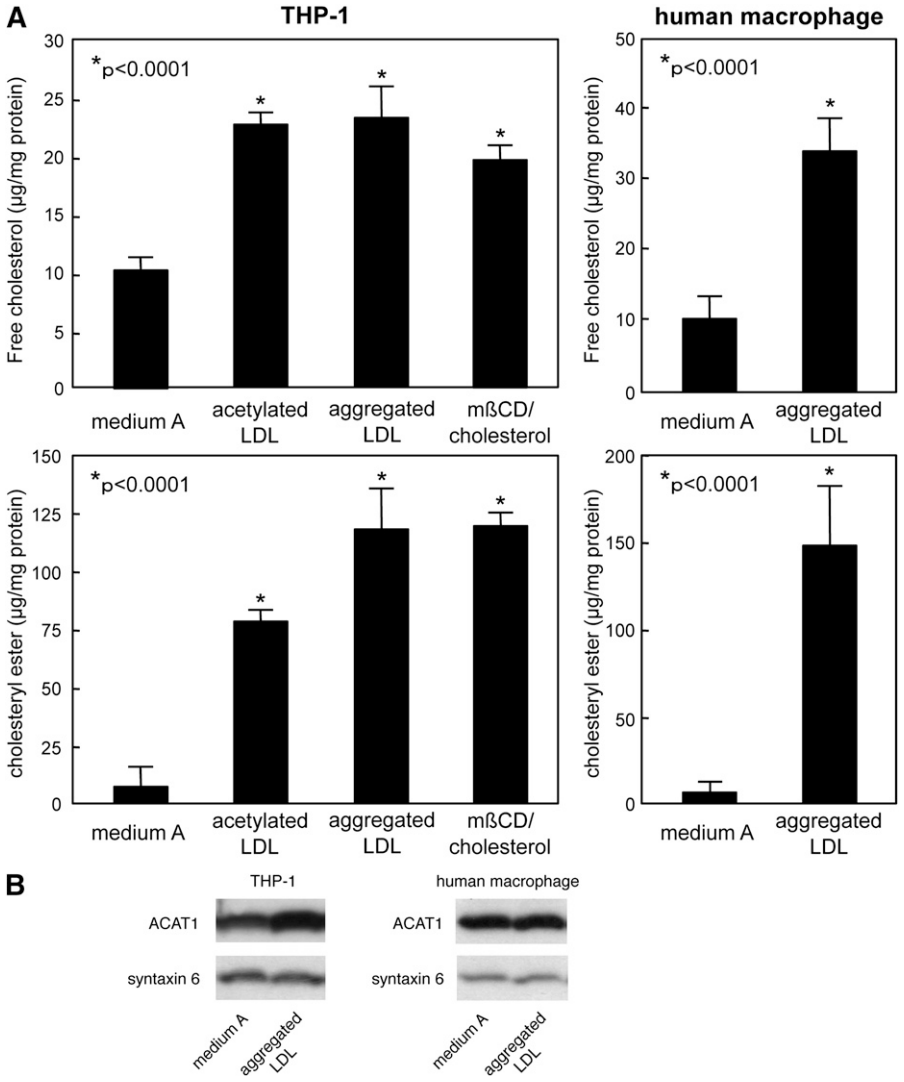

Fig. 1. Changes in cholesterol/cholesteryl ester content (A) and in expression levels of ACAT1 and syntaxin 6 (B) in macrophages. THP-1 macrophages (left panels) and human monocyte-derived macrophages (right panels) grown in medium A with or without aggregated LDL treatment for 48 h were subjected to cholesterol/cholesteryl ester mass analysis and immunoblot analysis as described in Methods, using whole cell lysates. Cholesterol/cholesteryl ester mass analysis was also carried out using THP-1 macrophages treated with acetylated LDL or with mβCD/cholesterol complex. Data are representative of two separate experiments.

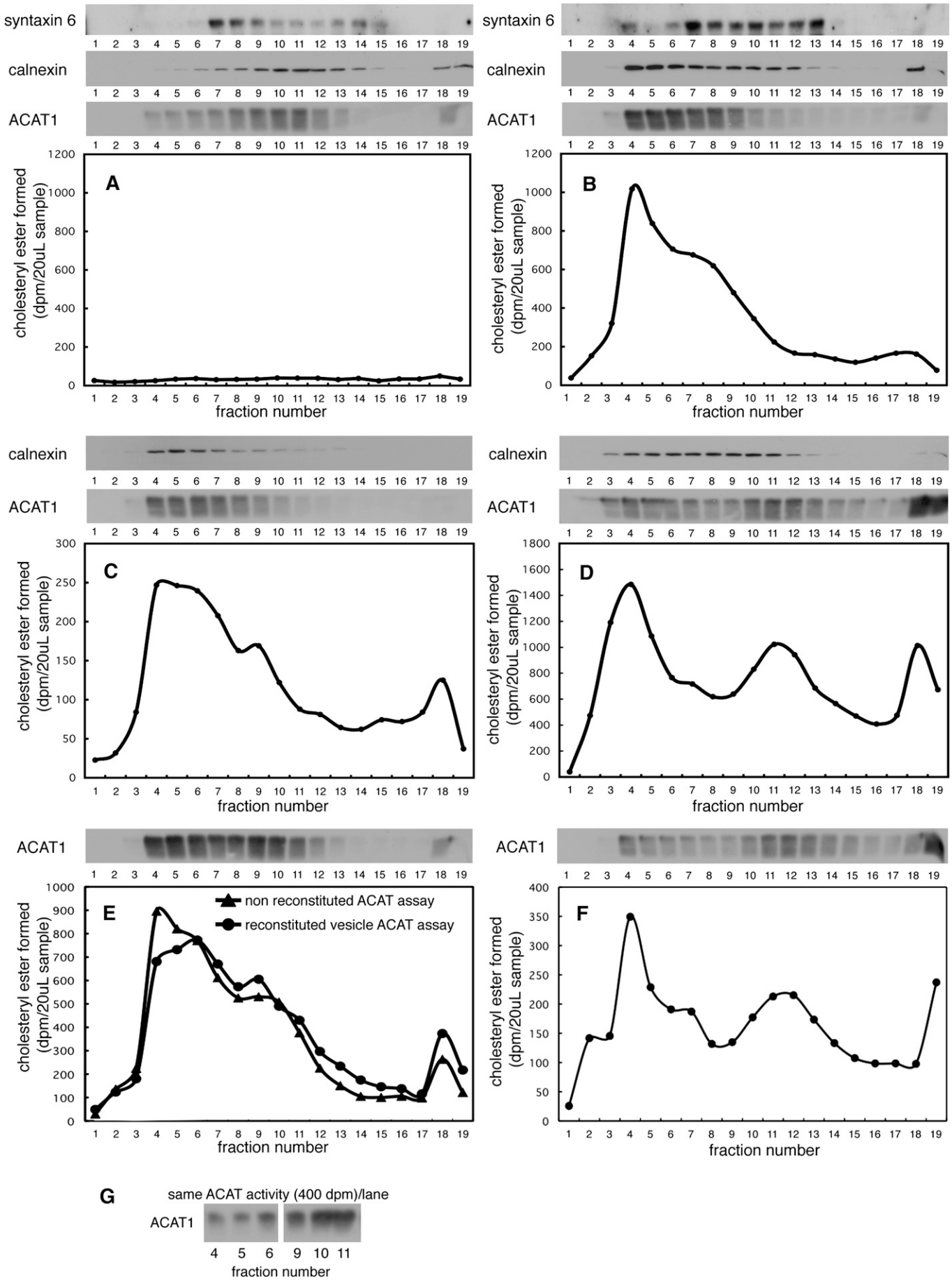

also moved to the lighter-density fractions (Fig. 2B). Similar changes in the densities of the ACAT1-containing membranes were observed when the THP-1 macrophages were treated for 2 days with 100 μg/ml of acetylated LDL (Fig. 2C) or with mβCD/cholesterol complex (Fig. 2D). We next examined the ACAT enzymatic activities in each of the OptiPrep membrane fractions shown in Fig. 2A–D by using the nonreconstituted assay (described in Methods). This assay uses cholesterol associated with each membrane fraction as the enzyme substrate. The results (Figs. 2A–D; lower panels) showed that in cells grown in basal conditions, the ACAT activities in various membrane fractions were very low (Fig. 2A); in cells treated with various cholesterol donors, the lighter-density membranes contained higher ACAT activity than the medium-density membranes (Figs. 2B–D). We also found that incubating the THP-1 macrophages with aggregated LDL for only 8 h is sufficient to produce the lower-density membranes with elevated ACAT activity (Fig. 2F). To test if the increase in ACAT activity in the less-dense membranes might be due to increases in cholesterol content in these membranes, we repeated the experiment shown in Fig. 2B and examined the ACAT activity in each fraction by using both the nonreconstituted assay and the reconstituted vesicle assay; the latter assay (described in Methods) uses cholesterol present in the reconstituted lipid vesicles as the enzyme substrate. The results (Fig. 2E) showed that the ACAT activities in the lower-density membranes remained elevated when exogenous cholesterol was used as the enzymatic substrate, demonstrating that the elevation in ACAT activity in these membranes is not caused by an increase in cholesterol content in these membranes. To evaluate the ACAT1 enzyme activity based on ACAT1 protein content, we repeated the experiment shown in Fig. 2B, loaded samples from OptiPrep fractions 4–6 and 9–11 that provided equal amount of ACAT activity in vitro, and compared their relative ACAT1 protein content by immunoblotting. The results (Fig. 2G) showed that at equal ACAT1 protein mass, the lower-density membrane fractions contained significantly higher ACAT enzymatic activity than the medium-density membrane fractions (by approximately 3-fold).

We also found that treating cell homogenates of macrophages grown in medium A with mβCD/cholesterol complex produced high ACAT enzyme activity in vitro but failed to produce the ACAT1-containing membranes that exhibited lesser density (results not shown). Also, treating THP-1 macrophages with aggregated LDL and with a specific chemical ACAT inhibitor still produced the same lighter-density ER-derived fraction, while the ACAT activities in these fractions were effectively inhibited (results not shown). Together, these data indicate that it is the increase in cellular cholesterol, not cellular cholesteryl ester, that produces the lighter-density membranes with elevated ACAT activity and that the action of cholesterol requires cellular integrity.

Immunofluorescent confocal microscopic analysis in THP-1 and primary human macrophages

We next employed confocal microscopy to monitor changes in ACAT1 localization in THP-1 (**Fig. 3A**, B, left panels) and primary human macrophages (Fig. 3A, B, right panels). The results show that in cells grown in medium A, ACAT1 signal was mainly located in the ER area; however, in cells treated with aggregated LDL, a significant amount of ACAT1 signal appeared in the juxtanuclear position (Fig. 3A, green). We next performed double immunofluorescence staining using ACAT1 antibodies or antibodies against syntaxin 6 (a protein mainly localized in the tubulovesicular element of TGN) (19). The results showed that in cells grown in medium A, only 6% apparent colocalization occurred between the ACAT1 signal and the Golgi marker (Fig. 3B, blue bars). In the cholesterol-rich macrophages, approximately 25% of the ACAT1 signal coincided with the Golgi marker (Fig. 3B, yellow bars). The colocalization coefficients between ACAT1 and syntaxin 6 are summarized in Fig. 3B. In cholesterol-rich cells, part of the ER protein marker BiP was also shifted to the juxtanuclear Golgi area and exhibited significant colocalization with the syntaxin 6 signal (results not shown). Additional experiments showed that in THP-1 macrophages grown in medium A with or without aggregated LDL, the ACAT1 signals extensively colocalized with the ER marker BiP signal (results not shown). To test if the findings made in THP-1 macrophages may also occur in human macrophages, we incubated human monocyte-derived macrophages in medium A or in medium A plus aggregated LDL for 2 days, then examined the ACAT1 localization by confocal microscopy. The results (Fig. 3A, B; right panels) showed that in medium A, the ACAT1 signal did not colocalize significantly with the syntaxin 6 signal, whereas in medium with aggregated LDL present, significant partial colocalization between these two signals occurred. The calculated colocalization coefficients between ACAT1 and syntaxin 6 are given in Fig. 3B, right panel. After cholesterol loading, the degree of apparent colocalization between the ER marker BiP and the TGN marker syntaxin 6 also increased (results not shown). Together, these observations suggest that in cholesterol-rich THP-1 macrophages or primary human

Fig. 2. Density and enzyme activity of ACAT1-positive membranes from THP-1 macrophages. Cells were grown in various media for 48 h. A, medium A; B, E, medium A plus 100 μg/ml aggregated LDL; C, medium A plus 100 μg/ml of acetylated LDL; and D, medium A plus 250 μM mβCD and 16 μM cholesterol complex. F: Medium A plus 100 μg/ml aggregated LDL for only 8 h. The homogenates were subjected to OptiPrep gradient ultracentrifugation; the ACAT1 protein content, ACAT enzyme activity, and various organelle marker proteins were determined by procedures described in Methods. E: ACAT activities determined by using both the nonreconstituted and the reconstituted vesicle assays; the assays were described in Methods. G: ACAT1 intensities in various OptiPrep fractions as analyzed by SDS-PAGE Western blotting. Aliquots from various fractions that produced the same amount of enzyme activity (400 dpm of labeled cholesteryl esters in ACAT enzyme assay) were loaded per lane. The results are representative of two experiments.

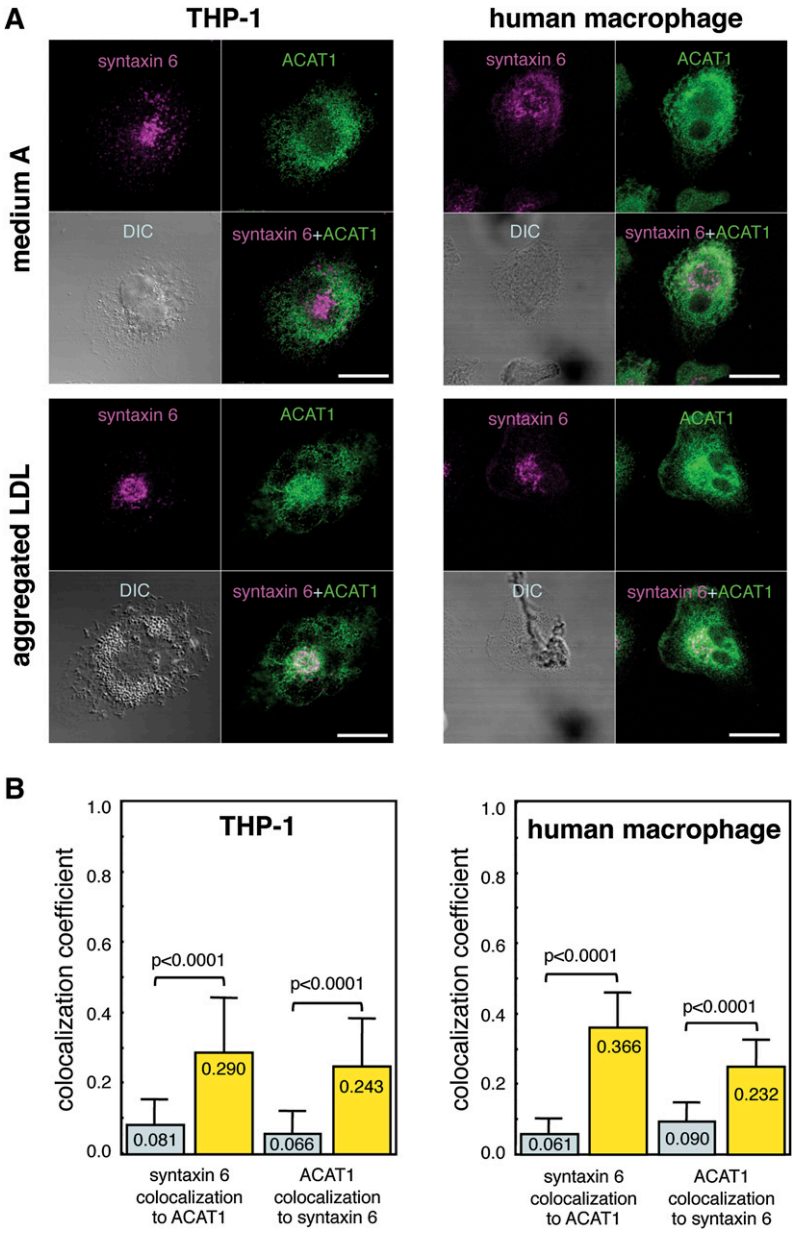

Fig. 3. Apparent colocalizations between ACAT1 and the Golgi marker (syntaxin 6) in THP-1 cells (left panels) or in primary macrophages (right panels). A: Cells with or without aggregated LDL treatment were viewed under confocal microscopy. Double immunofluorescent labeling was performed by using antibodies against ACAT1 or against the Golgi marker. B: Degree of apparent colocalization between ACAT1 and syntaxin 6. Blue bars are results without aggregated LDL; yellow bars are results with aggregated LDL. For each condition, more than 30 immunostained cells were randomly scanned; the colocalization coefficients were calculated from the scans. Scale bars in **A** are 20 μm. The results are representative of three separate experiments. DIC, Differential interference contrast.

macrophages, a significant amount of ACAT1 may be located near TGN.

The presence of syntaxin 6 in purified lower-density, ACAT1-positive membranes

To provide more evidence for a tight association of ACAT1 with a specific fraction of Golgi-related membrane(s), we first purified the ACAT1-positive, lower-density membranes in cholesterol-loaded THP-1 macrophages by OptiPrep gradient centrifugation; we then subjected the purified fractions to a second OptiPrep gradient centrifugation (described in Methods). After the second centrifugation step, the ACAT1-positive fractions remained in the lower-density fractions. The same fractions also contained the TGN marker syntaxin 6, the ER marker BiP, and the plasma membrane marker Na/K ATPase, but they lacked the *cis*-Golgi matrix marker GM130 (present in the higher-density fractions after the second centrifugation step) (**Fig. 4A**, upper panel). These ACAT1-positve fractions still retained high ACAT enzymatic activity in vitro (Fig. 4A, lower panel). After the second centrifugation, we analyzed the lipid contents present in various OptiPrep fractions. The lower-density fractions rich in ACAT enzyme activities were also rich in cholesterol and in cholesteryl esters (Fig. 4A, upper panel). Next, we further purified these ACAT1-positive vesicles after two-step subcellular fractionation by performing immunoadsorption using Pansorbin beads containing ACAT1 specific antibodies. After immunoadsorption, the samples were analyzed by Western blotting. The results show (Fig. 4B) that when ACAT1 antibodies were employed, the pelleted

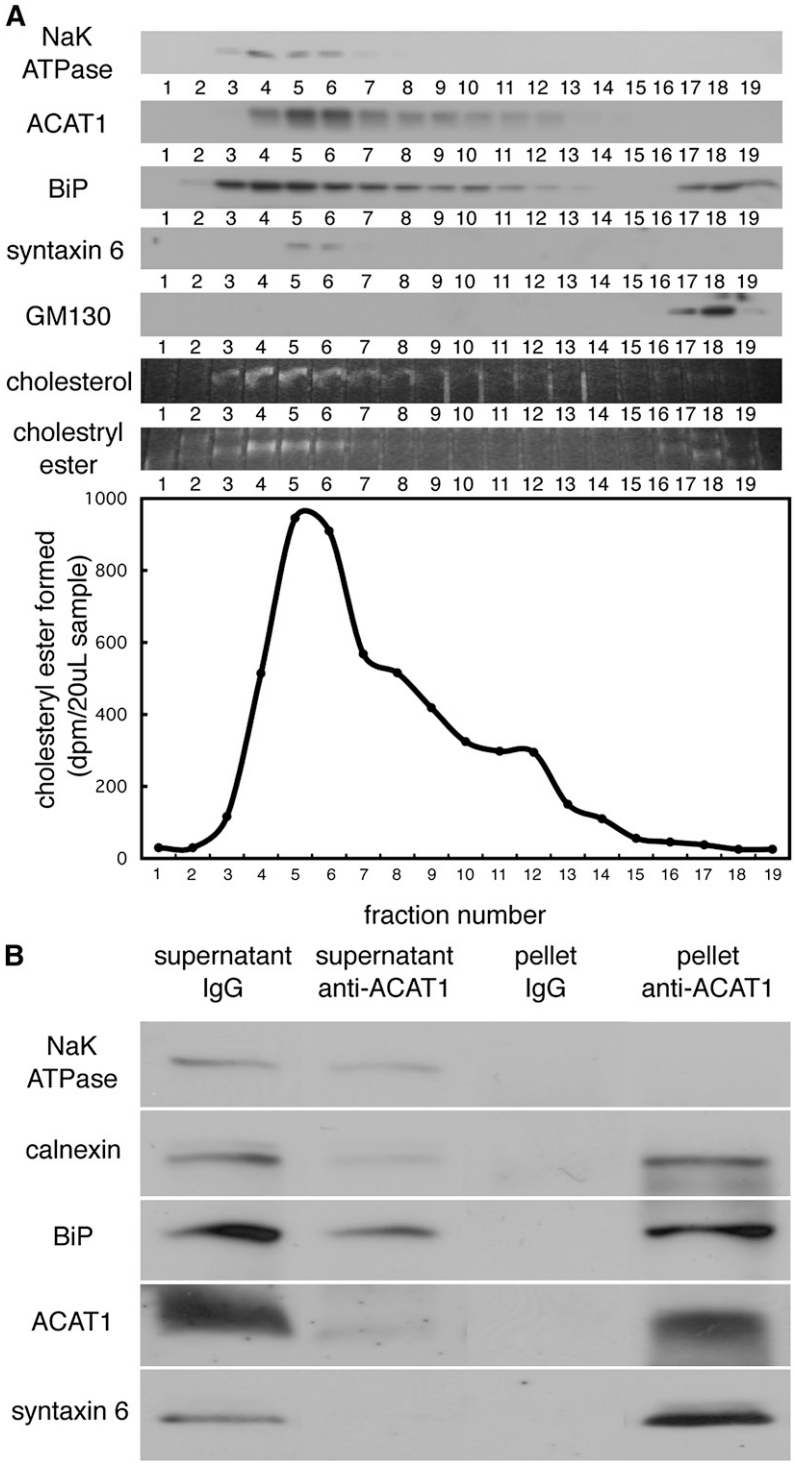

Fig. 4. Association of TGN marker with the ACAT1-positive membrane. A: Distribution of organelle marker proteins, cellular cholesterol/cholesteryl ester mass, and ACAT enzyme activity after a two-step fractionation. Homogenates of THP-1 macrophages treated with aggregated LDL were fractionated by a two-step procedure as described in Methods. The cholesterol/cholesteryl ester mass was isolated by lipid extraction and separated by TLC. The cholesterol and cholesteryl ester bands were visualized after staining with the lipid dye primulin. The ACAT enzyme activity determination was described in Methods. The results are representative of two separate experiments. B: Presence of syntaxin 6 in the purified ACAT1-positive membranes. After the two-step fractionation, the ACAT1-rich fractions were further purified by performing immunoadsorption using fractions 5 and 6 described in A as the starting material. Anti-ACAT1-specific Pansorbin beads (indicated as anti-ACAT1) or the nonimmune rabbit IgG beads (indicated as IgG) were used. The presence of various organelle markers in the immunoadsorbed pellet and in the immunodepleted supernatant was determined by immunoblot. The results are representative of two separate experiments.

membrane fraction contained ACAT1, the ER marker proteins (calnexin and BiP), and syntaxin 6, but it did not contain Na/K ATPase. When the nonimmunized rabbit IgG was employed as a negative control, none of the organelle markers were present in the pellet fraction. These results suggest that the highly purified ACAT1-positive membrane fraction is tightly associated with the ER marker proteins as well as the TGN marker protein syntaxin 6.

Biochemical analysis in primary human macrophages

To test the validity of findings made in THP-1macrophages, we grew human monocyte-derived macrophages in normal conditions (medium A) or in cholesterol-rich conditions (by incubating with 100 μg/ml of aggregated LDL for 48 h) and used these cells to perform similar experiments as described earlier. The results showed that when cells were grown in medium A, a small amount of ACAT1 as well as the ER marker calnexin and the TGN

marker syntaxin 6 were already detectable in lighter density fractions 4–6 (**Fig. 5A**). In cholesterol-rich conditions, more ACAT1 protein and more ER marker protein calnexin appeared in the lower-density fractions, and the ACAT1 protein present in these fractions exhibited higher enzyme activity in vitro (Fig. 5B). Lipid-laden human and mouse macrophages also express ACAT2 (20). We performed immunoblotting analysis and found that the lower-density membranes only contained the ACAT1 signal but not the ACAT2 signal (results not shown). To validate this finding, we employed an ACAT1-specific inhibitor called K-604. Compound K-604 preferentially inhibits ACAT1 over ACAT2 by more than 200-fold; at 1 μM, it inhibits 80% of the ACAT1 activity without inhibiting the ACAT2 activity. The results showed that K-604 used at 1 μM inhibited approximately 90% of the ACAT activity associated

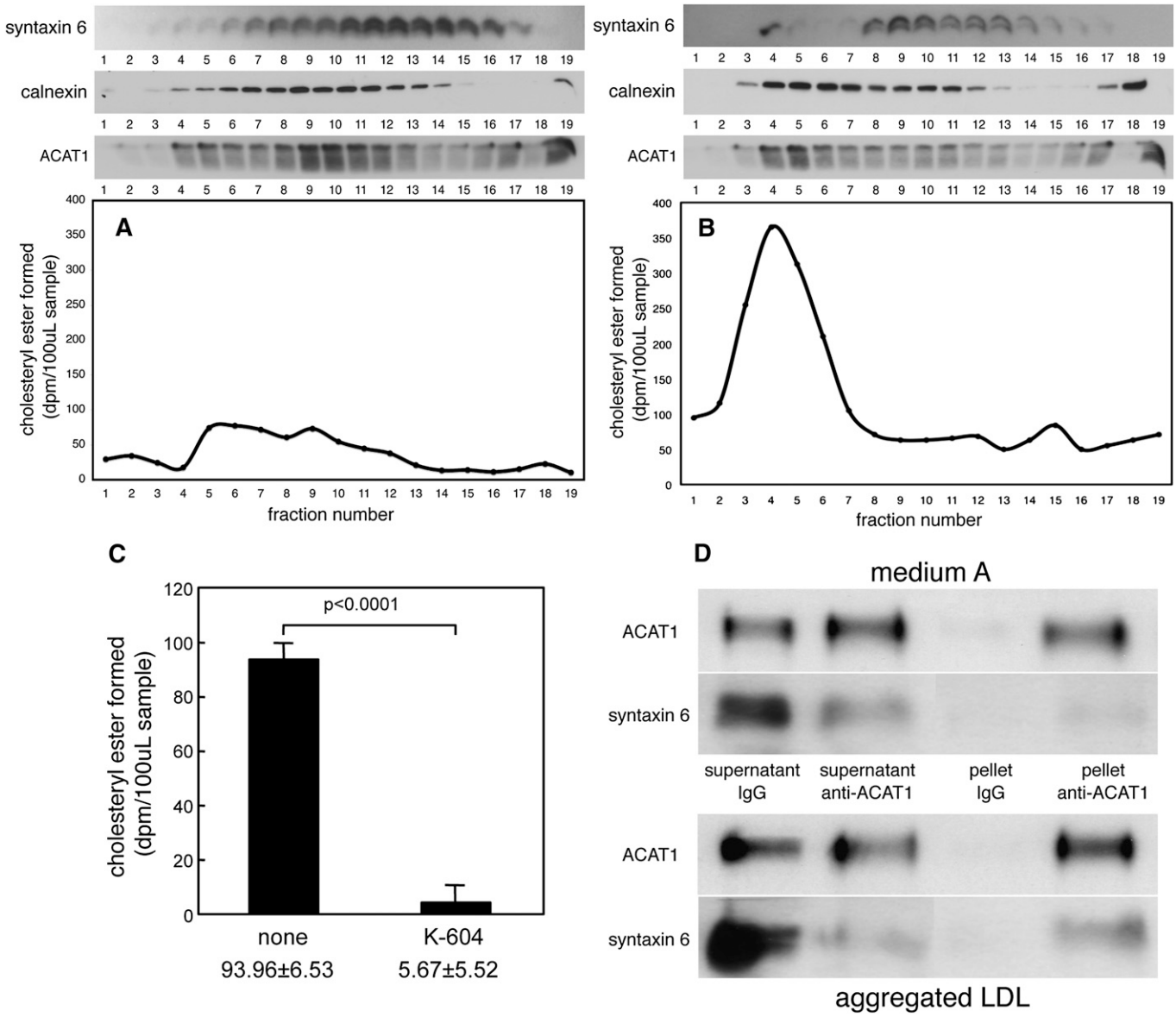

Fig. 5. The presence of ACAT1 in syntaxin 6-positive membranes in cholesterol-loaded human primary macrophages. A, B: The presence of ACAT1, the ER, and the TGN markers in lighter-density membranes after OptiPrep fractionation. Day 9 human primary macrophages grown in medium A without (A) or with (B) aggregated LDL for 48 h were subjected to subcellular fractionation and analyzed by western blot and by ACAT assay in vitro. The results are representative of two separate experiments. C: Inhibition of ACAT enzyme activity present in the lighter-density fractions by the ACAT1-specific inhibitor K-604. Human monocyte-derived primary macrophages treated with 100 μg/ml of aggregated LDL were subjected to subcellular fractionation; fractions 4–6 were combined and tested for inhibition by the ACAT1-specific ACAT inhibitor K-604 (at 1 μM final concentration) using the nonreconstituted ACAT assay. Final concentration of DMSO in each assay tube was kept at 0.1%. To serve as a negative control, ACAT enzyme activity was completely inactivated by adding SDS at 1% final concentration to the assay mixture. The data are representative of two separate experiments. D: The apparent association of TGN marker syntaxin 6 in ACAT1-positive membranes. Human macrophages incubated with (lower panel) or without (upper panel) aggregated LDL for 48 h were homogenized and the postnuclear supernatants were subjected to immunoadsorption using anti-human ACAT1-specific rabbit polyclonal antibodies (anti-ACAT1) or using nonimmunized rabbit IgG. The results are representative of two separate experiments.

with the lower-density membranes (Fig. 5C). These results demonstrate that the ACAT enzyme activity displayed in these lighter-density membranes mainly came from ACAT1, not ACAT2.

We next performed immunoadsorption experiments, using the postnuclear supernatants as the starting material. The results (Fig. 5D) showed that the ACAT1-positive membranes from cells in cholesterol-rich conditions were associated with the TGN marker syntaxin 6 (Fig. 5D, lower panels), while similar membranes from cells grown in medium A contained a negligible amount of syntaxin 6 (Fig. 5D, upper panels). These results confirm our previous results obtained in cholesterol-loaded THP-1 macrophages.

DISCUSSION

ACAT1 is located in the ER and ER-derived vesicles (12, 13). We had previously shown that upon loading macrophages with denatured LDL, there is an increase in the ER-derived, ACAT1-positive vesicles (13). To begin to pursue the biological significance of this finding, in the current manuscript, we first demonstrated that in macrophages, cholesterol itself (delivered as a soluble complex in cyclodextrin) could trigger the formation of the ER-derived vesicles. We next isolated these ER-derived vesicles in vitro and showed that the catalytic activity of ACAT1 present in these vesicles is increased; the increase in activity is not due to an increase in cholesterol content associated in these membranes. These results show that macrophages cope with cholesterol loading by using a novel mechanism: they produce more ER-derived vesicles that express elevated ACAT1 enzyme activity without having to produce more ACAT1 protein.

Currently, we do not know the mechanism(s) responsible for the cholesterol-dependent production of these ER-derived vesicles. We propose the following scenario as a starting point for future investigations: recent evidence suggests that ER membranes may be composed of various microdomains with distinct protein and lipid composition (21, 22). In various cell types, tubular ER and juxtanuclear ER-derived structures may coexist, with the tubular ER being the dominant form. Overloading of cholesterol in cells, especially in the macrophages, may somehow induce the formation of small, ER-derived vesicles, perhaps by an unknown ER fragmentation process. This process may allow the cholesterol-rich component of the ER to segregate from the rest of the ER, thus protecting the nonfragmented ER from being overloaded with cholesterol. ACAT1 present in the small, ER-derived vesicles may esterify cholesterol efficiently, preventing the accumulation of excess free cholesterol in cholesterol-rich subcellular organelles, including the TGN. This scenario is consistent with the hypothesis by Khelef et al. (12), who suggested that the proximity of the ACAT1-positive, ER-derived structure(s) with the cholesterol-rich organelles (TGN and endocytic recycling compartment) may provide a mechanism for localized control of cholesterol content of the ERC/TGN membranes. What causes the ACAT1 in the lower-density membranes to be more active than the ACAT1 in the higher-density ER membranes also remains unknown. It is possible that the higher-density ER membrane may contain an endogenous ACAT1 inhibitor and/or that the lower-density membranes may contain an endogenous ACAT1 activator. We are currently pursuing these possibilities.

We thank members of the T-Y.C. laboratory for discussion during the course of this work. We are also grateful to Helina H. Josephson and Stephanie Murphy for expert editing of this manuscript.

REFERENCES

1. Maxfield, F. R., and I. Tabas. 2005. Role of cholesterol and lipid organization in disease. *Nature.* **438:** 612–621.
2. Ikonen, E. 2008. Cellular cholesterol trafficking and compartmentalization. *Nat. Rev. Mol. Cell Biol.* **9:** 125–138.
3. Buhman, K. F., M. Accada, and R. V. Farese, Jr. 2000. Mammalian acyl-CoA:cholesterol acyltransferases. *Biochim. Biophys. Acta.* **1529:** 142–154.
4. Rudel, L. L., R. Lee, and T. Cockman. 2001. Structure, function, and regulation of ACAT. *Curr. Opin. Lipidol.* **12:** 121–127.
5. Chang, T. Y., B. L. Li, C. C. Chang, and Y. Urano. 2009. Acyl-coenzyme A:cholesterol acyltransferases. *Am. J. Physiol. Endocrinol. Metab.* **297:** E1–E9.
6. Parini, P., M. Davis, A. T. Lada, S. K. Erickson, T. L. Wright, U. Gustafsson, S. Sahlin, C. Einarsson, M. Eriksson, B. Angelin, et al. 2004. ACAT2 is localized to hepatocytes and is the major cholesterol-esterifying enzyme in human liver. *Circulation.* **110:** 2017–2023.
7. Song, B. L., C. H. Wang, X. M. Yao, L. Yang, W. J. Zhang, Z. Z. Wang, X. N. Zhao, J. B. Yang, W. Qi, X. Y. Yang, et al. 2006. Human acyl-CoA:cholesterol acyltransferase 2 gene expression in intestinal Caco-2 cells and in hepatocellular carcinoma. *Biochem. J.* **394:** 617–626.
8. Miyazaki, A., N. Sakashita, O. Lee, K. Takahashi, S. Horiuchi, H. Hakamata, P. M. Morganelli, C. C. Chang, and T. Y. Chang. 1998. Expression of ACAT1 protein in human atherosclerotic lesions and cultured human monocytes-macrophages. *Arterioscler. Thromb. Vasc. Biol.* **18:** 1568–1574.
9. Warner, G. J., G. Stoudt, M. Bamberger, W. J. Johnson, and G. H. Rothblat. 1995. Cell toxicity induced by inhibition of acyl coenzyme A:cholessterol acyltransferase and accumulation of unesterified cholesterol. *J. Biol. Chem.* **270:** 5772–5778.
10. Tabas, I. 2002. Consequences of cellular cholesterol accumulation: basic concepts and physiological implications. *J. Clin. Invest.* **110:** 905–911.
11. Chang, T. Y., C. C. Y. Chang, and D. Cheng. 1997. Acyl-coenzyme A:cholesterol acyltransferase. *Annu. Rev. Biochem.* **66:** 613–638.
12. Khelef, N., T. T. Soe, O. Quehenberger, N. Beatini, I. Tabas, and F. R. Maxfield. 2000. Enrichment of acyl coenzyme A:cholesterol O-acyltransferase near trans-golgi network and endocytic recycling compartment. *Arterioscler. Thromb. Vasc. Biol.* **20:** 1769–1776.
13. Sakashita, N., A. Miyazaki, M. Takeya, S. Horiuchi, C. C. Y. Chang, T. Y. Chang, and K. Takahashi. 2000. Localization of human acyl-coenzyme A:cholesterol acyltransferase-1 in macrophages and in various tissues. *Am. J. Pathol.* **156:** 227–236.
14. Chang, C. C. Y., J. Chen, M. A. Thomas, D. Cheng, V. A. Del Priore, R. S. Newton, M. E. Pape, and T. Y. Chang. 1995. Regulation and immunolocalization of acyl-coenzyme A: cholesterol acyltransferase in mammalian cells as studied with specific antibodies. *J. Biol. Chem.* **270:** 29532–29540.
15. Chang, C. C., C. Y. Lee, E. T. Chang, J. C. Cruz, M. C. Levesque, and T. Y. Chang. 1998. Recombinant acyl-CoA:cholesterol acyltransferase-1 (ACAT-1) purified to essential homogeneity utilizes

cholesterol in mixed micelles or in vesicles in a highly cooperative manner. *J. Biol. Chem.* **273:** 35132–35141.
16. Ikenoya, M., Y. Yoshinaka, H. Kobayashi, K. Kawamine, K. Shibuya, F. Sato, K. Sawanobori, T. Watanabe, and A. Miyazaki. 2007. A selective ACAT-1 inhibitor, K-604, suppresses fatty streak lesions in fat-fed hamsters without affecting plasma cholesterol levels. *Atherosclerosis.* **191:** 290–297.
17. Huang, W., I. Ishii, W-Y. Zhang, M. Sonobe, and H. S. Kruth. 2002. PMA activation of macrophages alters macrophage metabolism of aggregated LDL. *J. Lipid Res.* **43:** 1275–1282.
18. Cadigan, K. M., and T. Y. Chang. 1988. A simple method for reconstitution of CHO cell and human fibroblast ACAT activity into liposomes. *J. Lipid Res.* **29:** 1683–1692.
19. Bock, J. B., J. Klumperman, S. Davanger, and R. H. Scheller. 1997. Syntaxin 6 functions in trans-Golgi network vesicle trafficking. *Mol. Biol. Cell.* **8:** 1261–1271.
20. Sakashita, N., A. Miyazaki, C. C. Y. Chang, P. Morganelli, T. Y. Chang, O. Nakamura, E. Kiyota, H. Hakamata, M. Satoh, H. Tamagawa, et al. 2003. The presence of ACAT2 in human and mouse macrophages: in vivo and in vitro studies. *Lab. Invest.* **83:** 1569–1581.
21. Baumann, O., and B. Walz. 2001. Endoplasmic reticulum of animal cells and its organization into structural and functional domains. *Int. Rev. Cytol.* **205:** 149–214.
22. Shibata, Y., G. K. Voeltz, and T. A. Rapoport. 2006. Rough sheets and smooth tubules. *Cell.* **126:** 435–439.